

**A REVIEW: COMPUTATIONAL MODELING AND SIMULATION OF  
DOWNDRAFT BIOMASS GASIFIER**Rahul Gupta<sup>1</sup>, Pankaj Jain<sup>2</sup>, Savita Vyas<sup>3</sup><sup>1</sup>Student of School of Energy & Environment Mgmt. RGPV, Bhopal, India<sup>2,3</sup>Asst. Professor of School of Energy & Environment Mgmt. RGPV, Bhopal, India

**ABSTRACT:** Biomass is the clean energy source which is indirectly solar energy form. Biomass gasification is the ecofriendly and alike clean technology for recent which convert solid biomass into gaseous fuel (CH<sub>4</sub>, CO<sub>2</sub>, H<sub>2</sub> etc.). Biomass energy conversion combined with computation fluid dynamics (CFD) software has been delineated in some detail within the following review paper. Biomass gasification involves complicated reaction pathways, reactive gas-particle behavior, and comminution of solid biomass particles. modeling and simulation as CFD (computational fluid dynamics) are playing important role in our study and analysis because of CFD gives insight into flow pattern that is difficult, expensive or impossible to study using EFD (Experimental fluid dynamics). Various type of biomass gasification models thermodynamic equilibrium, kinetic and artificial neural network etc. shows and analyzed in this paper. A CFD software package is used for the basic computational model. Advanced computer visualization techniques are used to observe the fluid flow pattern and reduction of solid biomass particles in the gasifier. The effects of gasifier configuration, temperature, steam/biomass ratio, and biomass/bed material ratio, biomass loading rate and yield biomass particle size and composition of syngas are analyzed by use of the CFD model.

**Keyword-** CFD, EFD, pathway, fluid flow pattern, artificial neural network, biomass, gasification

**I. INTRODUCTION**

World has large energy demands and difficult to fulfill those needs through non-renewable energy technology is increasing daily. Due to raise in energy demand and fuel depletion the alternate sources like wind, solar, biomass, and fuel cell were being progressively utilized. Biomass is presently the most important supply of renewable energy, accounting for approximately 10-15% (or  $45 \pm 10$  EJ) of the world's total energy provide[1]. About 32% of the total primary energy consume in the country is still derived from biomass and more than 70% of the country's population depends upon it for its energy need.[2] biomass is an organic matter which is derived from plant and animal material such as wood, forestry waste, leave, and agriculture waste like husk and straw etc. biomass gasification is a exothermic conversion reaction of biomass into the gaseous fuel which is high grade and quality of fuel rather than solid biomass fuel. Total renewable power production in India has the potential of 17,538 MW of biomass. The numerical simulation and modeling techniques such as CFD turn out to be a reality and offer an effective means of quantifying the physical and chemical process in the biomass thermochemical reactors under different operating conditions within a virtual environment.[3]

**II. GASIFICATION AND GASIFICATION PROCESS**

Gasification is thermochemical conversion process to convert the low grade fuel such as coal, biomass etc. into the high grade and clean fuels like synthetic gas or producer gas. The whole reaction takes place in the gasifier. The chemistry of biomass gasification is quite complex. Broadly speaking, the gasification process involves of the following phase/zone:[4-6]

- **DRYING:** In this stage, the moisture content of the biomass is reduced. Typically, the moisture content of biomass ranges from 5% to 35%. Drying occurs at about 100–200°C with a reduction in the moisture content of the biomass of <5%.
- **DEVOLATILISATION (PYROLYSIS):** This is essentially the thermal decomposition of the biomass in the absence of oxygen or air. In this process, the volatile matter in the biomass is reduced. This results in the release of hydrocarbon gases from the biomass, due to which the biomass is reduced to solid charcoal. The hydrocarbon gases can condense to form liquid tars at a sufficiently low temperature.
- **OXIDATION:** This is a reaction between solid carbonized biomass and oxygen in the air, resulting in the formation of CO<sub>2</sub>. Hydrogen existing in the biomass is also oxidized to produce water. A large amount of heat is dissipated with the oxidation of carbon and hydrogen. If oxygen is present in substoichiometric quantities, partial oxidation of carbon may occur, resulting in the generation of carbon monoxide.

- **REDUCTION:** In the absence (or sub stoichiometric presence) of oxygen, several reduction reactions occur in the 800–1000°C temperature range. These reactions are mostly endothermic. The process of gasification of biomass shown the figure (1)

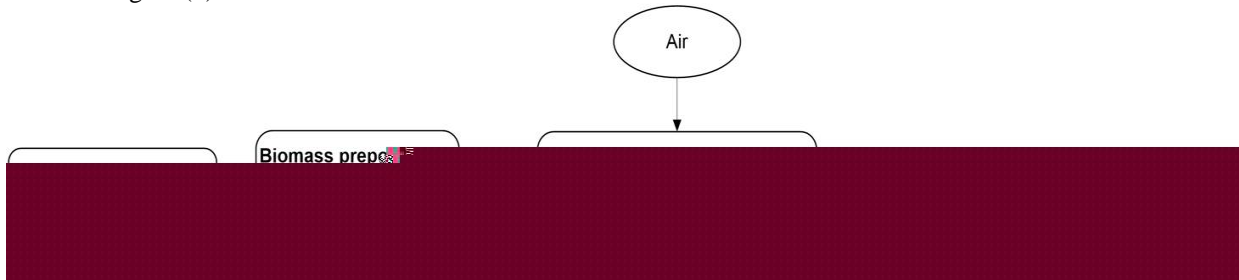


*Figure 1. Process chart of gasification of biomass*

**Type of biomass gasifier:**

- 1) Fixed bed gasifier-
  - a) Updraft gasifier
  - b) Downdraft gasifier
  - c) Cross bed gasifier
- 2) Fluidized bed gasifier
  - a) Circulating bed gasifier
  - b) Bubbling bed gasifier
  - c) Circulating and bubbling bed gasifier

**Downdraft gasifier:** Biomass fuel is feed from the top and moves downward. Oxidant agent (air) is introduced at the top and flows downward. Synthesis gas is extracted at the bottom at grate level. **Updraft gasifier:** Biomass fuel is introduced from the top and moves downward. Oxidant agent is introduced at the bottom and flows upward. Some drying occurs. Synthesis gas is extracted at the top. **Cross draft gasifier:** Biomass fuel is put from the top and moves downward. Oxidant agent is introduced at the bottom and flows across the bed. Synthesis gas is blowout opposite the air nozzle at the grate. **Fluidize bed gasifier:** Air is introduced through a solid particles bed at a sufficient velocity to keep these in a state of suspension and behave as fluid. This velocity is known as fluidized velocity. The fuel particles are feed at the bottom of the reactor, very quickly blended with the bed material and almost rapidly heated up to the bed temperature. As a consequence of this treatment the fuel is pyrolysis very fast, resulting in a component blend with a relatively large amount of gaseous materials. Further gasification and tar-conversion reactions take place in the gas phase.

Down-draft gasifiers have comparatively low tar content and therefore generally are the preferred type for small scale power generation from biomass. it should also be realized that the tar from downdraft gasifiers is more stable than from updraft gasifiers, which may still provide problems in tar elimination. In updraft gasifier there is a problem of tar entrainment in the producer gas exit stream, a solution is to have primary gasification air blown at or above the oxidation zone in the gasifier. The produced gas is flown out from the bottom hence fuel and gas travel in the same direction. Systematic diagram of downdraft gasifier shown below

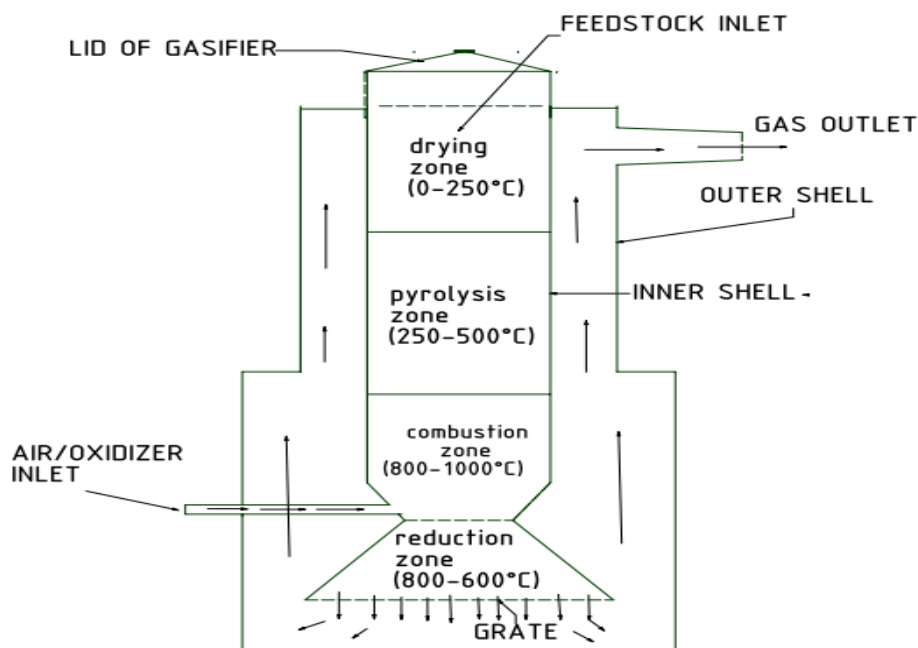


*Figure 2. Downdraft gasifier*

### **III. COMPUTATIONAL FLUID DYNAMICS (CFD)**

Computational fluid dynamics may have a very important role in the modeling of biomass downdraft gasifier. A few works have been carried out in numerical and mathematical studies about gasification process using CFD technique.

#### **3.1.Theoretical considerations on CFD**

The CFD codes are prepared by the numerical algorithm accordingly so that the fluid flow problem can be tackled. There are three main elements of CFD codes in the CFD packages which involve pre-processor, solver, and post-processor.

##### **3.1.1.Pre-processor**

The pre-processor contains all inputs of the fluid flow for a flow problem. It can be seen as a user-friendly interface and a conversion of all the input into the solver in CFD program. In this phase, quite a lot of activities are carried out before the problem is being solved. These stages are listed as below:

- Definition of the geometry: The region of interests which is the computational domain.
- Grid generation: The subdivision of the domain into a number of smaller and no overlapping domains. The grid mesh of cells is carried out for the geometry.
- Selection of the physical and chemical properties: The geometry to be modeled.
- Definition of the fluid properties
- Specifications of correct boundary conditions: This is done at model's cells. The solution of the flow problem such as temperature, velocity, pressure etc. is defined at the nodes inside each cell. The accuracy of the CFD solution governed by the number of cells in the grid and is dependent on the fineness of the grid.

##### **3.1.2.Solver**

In the numerical solution technique, there are three various streams that form the basis of the solver. There are finite differences, finite element, and finite volume methods. The variations between them are the way in which the flow variables are approximated and the discretization processes are done.

###### **1. Finite difference element,**

FDM delineate the unknown flow variables of the flow problem by means of point samples at node points of a grid coordinate. By FDM, the Taylor's expansion is basically used to generate finite differences approximation.

###### **2. Finite element method,**

FEM use the basic piecewise functions valid on elements to detail the local variations of unknown flow variables. Governing equation is precisely satisfied by the exact solution of flow variables. In FEM, the errors are measured by using residuals.

###### **3. Finite volume method,**

It was primitively developed for special finite difference formulation. The main codes of computational commercial CFD packages using the finite volume method (FVM) approaches involve PHOENICS, FLUENT, FLOW 3D and STAR-CD. Generally, the numerical algorithm in these CFD commercial packages engaged the formal integration of the governing equation over all the finite control volume, the discretization process includes the substitution of multiplicity FDM types to approximate the integration equation of the flow problem and the solution is obtained by the iterative method. Discretization in the solver includes the approaches to solving the numerical integration of the flow problem. Usually, two different approaches have been used and once at a time.

- Explicit approach
- Implicit approach

##### **3.1.3.Post-processor**

A FLUENT package makes adequate preparation for the data visualization tools to visualize the flow problem. This includes – vectors plots, domain geometry and a grid display, line and shaded contour plots, particle tracking etc. Recent facilities aided with animation for show the dynamic result and also have data export facilities for further manipulation external to the code.

#### **3.2.Problem solving**

In the computational fluid dynamic, using the FLUENT codes help to solve the problem numerically. The fundamental involves determining the convergence, whether the solution is consistent and stable for all range of flow variables.

- Convergence – it is a property of a numerical method to produce a solution that approaches the exact solution of which the grid spacing, control volume size is reduced to a specific value or to zero value.
- Consistent – use to produce the system of algebraic equations which can be equivalent to the original governing equation.
- Stability – associates with the damping of errors as numerical method proceeds. Unless a technique chosen is stable, even the round-off error in the initial data can lead to wild oscillations or deviations.[7]



Figure 3. Process of CFD Modeling and Simulation

#### IV. DESCRIPTIONS OF MATHEMATICAL MODEL

##### 4.1. Basic governing equations

The equation for mass flow, momentum, and energy is given by following:

$$\nabla(\rho v) = S_m \quad (1)$$

$$\nabla \cdot (\rho v v) = \rho v v - \rho g + \nabla \cdot (\tau) + S_f \quad (2)$$

$$\nabla(v(\rho E + p)) = \nabla \cdot K \Delta T - \nabla \sum h_i J_i + \nabla \cdot (\tau \cdot v) \quad (3)$$

Where, K is the effective conductivity and  $J_i$  is the diffusion of species i.

##### 4.2. Turbulence model:-

Turbulent flows are followed by fluctuating velocity fields primarily due to the complicated geometry and/or high flow rates. Turbulence affects the heat and mass transfer and plays an essential role in some processes such as biomass gasification/devolatilization in fluidized bed and non-premixed combustion in furnaces and combustion chamber etc. The Navier-Stokes equations can be solved directly for laminar flows, but for turbulent flows the direct numerical simulation (DNS) with full solution of the transport equations at all length and time scales is too computationally expensive since the fluctuations can be of small scale and high frequency.[3]

Most common RANS turbulence model applied to pulverized combustion is k-epsilon and its variants (standard and Realizable). The k-epsilon models provide a good solution without excessive computation time. Realizable k-epsilon model generally performs better than standard k-epsilon model in predicting swirling combustion flows[8]

##### 4.2.1. Standard k-epsilon model:-

The simplest “complete models” of turbulence are two-equation models in which the solution of two separate transport equations allows the turbulent velocity and length scales to be individually determined. The standard k-model in CFD FLUENT categories in this class of turbulence model and has come to be the workhorse of practical engineering flow calculations in the time since it was proposed by Launder and Spalding. In the standard k-epsilon model, the k and epsilon can be achieved from the following transport equations as[9]

$$\frac{\partial}{\partial t}(\rho k) + \frac{\partial}{\partial x_i}(\rho k u_i) = \frac{\partial}{\partial x_j} \left[ \left( \mu + \frac{\mu_t}{\sigma_k} \right) \frac{\partial k}{\partial x_j} \right] + G_k + G_b - \rho \epsilon - Y_M + S_k \quad (4)$$

And

$$\frac{\partial}{\partial t}(\rho \epsilon) + \frac{\partial}{\partial x_i}(\rho \epsilon u_i) = \frac{\partial}{\partial x_j} \left[ \left( \mu + \frac{\mu_t}{\sigma_k} \right) \frac{\partial \epsilon}{\partial x_j} \right] + C_{1\epsilon} \frac{\epsilon}{k} (G_k + C_{3\epsilon} G_b) - C_{2\epsilon} \rho \frac{\epsilon^2}{k} + S_\epsilon \quad (5)$$

In these equations,  $G_k$  indicates the generation of turbulence kinetic energy due to the mean velocity gradients,  $G_b$  represent the generation of turbulence kinetic energy due to buoyancy,  $Y_M$  represents the contribution of the fluctuating dilatation in compressible turbulence to the overall dissipation rate,  $C_1$ ,  $C_2$ , and  $C_3$  are constants.  $\sigma_k$  and  $\sigma_\epsilon$  are the turbulent Prandtl numbers for k and epsilon, respectively.  $S_k$  and  $S_\epsilon$  are user-defined source terms

Modeling the Turbulent Viscosity The turbulent (or eddy) viscosity,  $\mu_t$ , is computed by combining k and epsilon as follows:  $\mu_t =$

$$\rho C_\mu \frac{k^2}{\epsilon} \quad (6)$$

Where,  $C_\mu$  is a constant

#### 4.2.2. RNG k-ε model

The RNG-based k-ε turbulence model is consequent from the rapid Navier-Stokes equations, using a mathematical technique called “renormalization group” (RNG) methods. The analytical derivation results in a model with constants different from those in the standard k-ε model, and additional terms and functions in the transport equations for k and ε. A more inclusive description of RNG theory and its application to turbulence can be found in. The RNG k-ε model has a similar form to the standard k-ε model:

$$\frac{\partial}{\partial t}(\rho k) + \frac{\partial}{\partial x_i}(\rho k u_i) = \frac{\partial}{\partial x_j} \left( \alpha_k \mu_{eff} \frac{\partial k}{\partial x_j} \right) + G_k + G_b - \rho \epsilon - Y_M + S_k \quad (7)$$

and

$$\frac{\partial}{\partial t}(\rho \epsilon) + \frac{\partial}{\partial x_i}(\rho \epsilon u_i) = \frac{\partial}{\partial x_j} \left( \alpha_\epsilon \mu_{eff} \frac{\partial \epsilon}{\partial x_j} \right) + C_{1\epsilon} \frac{\epsilon}{k} (G_k + C_{3\epsilon} G_b) - C_{2\epsilon} \rho \frac{\epsilon^2}{k} - R_\epsilon + S_\epsilon \quad (8)$$

The quantities  $\alpha_k$  and  $\alpha_\epsilon$  are the inverse effective Prandtl numbers for k and ε respectively.

$$R_\epsilon = \frac{C_{\mu} \rho \eta^3 \left(1 - \frac{\eta}{\eta_0}\right) \epsilon^2}{1 + \beta \eta^3} \frac{1}{k} \quad (9)$$

#### 4.2.3. Realizable k-ε model

Both the realizable and RNG k-ε models have shown considerable improvements over the standard k-ε model where the flow topographies include strong streamline curvature, vortices, and rotation. Since the model is still relatively new, it is not clear in exactly which instances the realizable k-ε model consistently outperforms the RNG model.[10]

$$\frac{\partial}{\partial t}(\rho k) + \frac{\partial}{\partial x_i}(\rho k u_i) = \frac{\partial}{\partial x_j} \left[ \left( \mu + \frac{\mu_t}{\sigma_k} \right) \frac{\partial k}{\partial x_j} \right] + G_k + G_b - \rho \epsilon - Y_M + S_k \quad (10)$$

$$\frac{\partial}{\partial t}(\rho \epsilon) + \frac{\partial}{\partial x_i}(\rho \epsilon u_i) = \frac{\partial}{\partial x_j} \left( \alpha_\epsilon \mu_{eff} \frac{\partial \epsilon}{\partial x_j} \right) \rho C_{1\epsilon} S_\epsilon - \rho C_{2\epsilon} \frac{\epsilon^2}{k + \sqrt{\nu \epsilon}} + C_{1\epsilon} \frac{\epsilon}{k} C_{3\epsilon} G_b + S_\epsilon \quad (11)$$

Where

$$C_1 = \max \left[ 0.43, \frac{\eta}{\eta + 5} \right], \eta = S \frac{k}{\epsilon}, S = \sqrt{2 S_{ij} S_{ij}}$$

$C_1$  &  $C_2$  are constant

#### 4.3. Species transport CFD model

The species transport model has been selected to model the chemical reactions inside the gasifier and to find out the composition of various species like CO, CO<sub>2</sub>, N<sub>2</sub>, H<sub>2</sub> and CH<sub>4</sub>. The standard equations used in this process are discussed below. The chemical reactions are solved by the conservation equations relating to convection, diffusion and reaction of each species. The general form of the transport equation for each species is defined as[11]

$$\frac{\partial}{\partial t}(\rho Y_i) + \nabla \cdot (\rho \vec{v} Y_i) = \nabla \cdot \vec{J}_i + R_i \quad (12)$$

The species transport equations for each species is obtained by substituting the appropriate variable for the terms in the above equation.

“ $R_i$ ” is the net rate of production of species “i” by chemical reaction. “ $J$ ” is the diffusion flux of species “i” which arises due to concentration gradients. Mass diffusion for laminar flows is given as

$$\vec{J} = - \left( \rho D_{i,m} + \frac{\mu_i}{Sc_i} \right) \nabla Y_i \quad (13)$$

For turbulent flows, mass diffusion flux is given by

$$\vec{J} = - \rho D_{i,m} \nabla Y_i \quad (14)$$

Where  $D_{i,m}$  is the mass diffusion coefficient of species in the mixture, and  $Sc_i$  is the turbulent Schmidt number. The rate of chemical reaction is computed using an expression that accounts for the temperature and pressure by ignoring the effects of the turbulent eddies. The net rate of production or destruction of species i as the result of reaction r, in  $R_{i,r}$  is given by

$$R_{i,r} = v'_{i,r} M_{i,r} A \rho \frac{\epsilon}{k} \min_g \left( \frac{Y_r}{v'_{i,r} M_{w,j}} \right) \quad (15)$$

$$R_{i,r} = v'_{i,r} M_{i,r} B \rho \frac{\epsilon}{k} \min_g \left( \frac{\sum_P Y_P}{\sum_j^N v'_{i,r} M_{w,j}} \right) \quad (16)$$

Where  $Y_p$  is denote the mass fraction of any product species, P,  $Y_r$  is denote the mass fraction of a particular reactant, R

**4.4. Radiation model**

Radiation model: in This model, Radiative transfer equation (RTE) for an absorbing, emitting, and scattering medium at position  $r$  in the direction  $s$  can be given as[12]

$$\frac{dI(\vec{r},\vec{s})}{ds} + (\alpha + \sigma_s)I(\vec{r},\vec{s}) = an^2 \frac{\sigma T^4}{\pi} + \frac{\sigma_s}{4\pi} \int_0^{4\pi} I(\vec{r},\vec{s}')\Phi(\vec{r},\vec{s}')d\Omega \tag{17}$$

There are four common radiation models in Fluent

- P-1 Radiation Model
- Rosseland Model
- Discrete Ordinates Model (DOM)
- Discrete Transfer Radiation Model (DTRM)

**4.5. Kinetics of chemical reaction model**

Chemical reactions in Biomass gasification model are involved following process: Devolatilization of biomass, homogenous reaction and heterogeneous reaction.

The single-step global reaction for Devolatilization of biomass is defined as follows:



The reaction rate is described by the Arrhenius equation

$$r_p = k_p C_{bio} \tag{18}$$

$$K_p = fAT^n \exp\left(\frac{E_a}{RT}\right) \tag{19}$$

Where  $r_p$  is the rate of reaction of Devolatilization

$C_{bio}$  is the concentration of unreacted biomass particles,

$R$  is the universal gas constant,

$f$  is the fitting factor for pyrolysis reaction,

$n$  is the exponent of the reaction temperature;

$A$ , the pre-exponential factor, and  $E_a$ , the activation energy (99.0 s<sup>-1</sup> and 11.14 kJ/mol)[13]

**Heterogeneous char reactions:** In this study, the heterogeneous char reactions are:



**Homogeneous gas-phase reactions:** The following various homogeneous reactions are included in this study:



**Table 1. Kinetic Data of Heterogeneous Reactions[14, 15]**

Reaction	A (kg/m <sup>2</sup> ·s·Pa)	E/R (K)
R2	1.0 × 10 <sup>-3</sup>	3000
R3	6.35 × 10 <sup>-3</sup>	19500
R4	2.0 × 10 <sup>-2</sup>	8240
R5	1.18 × 10 <sup>-5</sup>	17 921

Table 2. Kinetic Data of Homogeneous Reactions[16, 17]

Reaction	Reaction rate eqs. (kmol/m <sup>3</sup> )	
R6	$r_6 = A_6 \exp(-E_6/RT)[CO][O_2]^{0.25}[H_2O]^{0.5}$	
R7	$r_7 = A_7 \exp(-E_7/RT)[H_2][O_2]$	
R8	$r_8 = A_8 T^{-1} \exp(-E_8/RT)[CH_4][O_2]$	
R9	$r_9 = A_9 \exp(-E_9/RT)[C_2H_4][O_2]$	
R10	$r_{10} = A_{10} \exp(-E_{10}/RT)([CO][H_2O] - ([CO_2][H_2])/K_{eq});$ $K_{eq} = 0.0265 \exp(3968/T)$	
Reaction	A	E(kj/mol)
R6	$2.32 \times 10^{12} (\text{kmol}/\text{m}^3)^{-0.75} \text{ s}^{-1}$	167
R7	$1.08 \times 10^{13} (\text{kmol}/\text{m}^3)^{-1} \text{ s}^{-1}$	125
R8	$5.16 \times 10^{13} (\text{kmol}/\text{m}^3)^{-1} \text{ s}^{-1} \text{ k}$	130
R9	$1.0 \times 10^{12} (\text{kmol}/\text{m}^3)^{-1} \text{ s}^{-1}$	173
R10	$12.6 (\text{kmol}/\text{m}^3)^{-1} \text{ s}^{-1}$	2.78

### V. LITERATURE REVIEW

In this review article investigate the different CFD Mathematical and simulation model of biomass gasifier given by various researchers.

Janajreh, I. and M. Al Shrah (2013)[18] investigate the numerical and experimental analysis of downdraft gasifier using wood chips. Numerical simulation using CFD to model the Lagrangian particle and conducted on a high resolution mesh accounting for the solid and gaseous phases,  $k-\epsilon$  turbulence, and reacting CFD model. In this model temperature distribution and species evolution compare with experimental data. The average temperature computed by CFD was higher compared to that measured experimentally and comparable to the calculated ideal one which corresponds to equilibrium conditions.

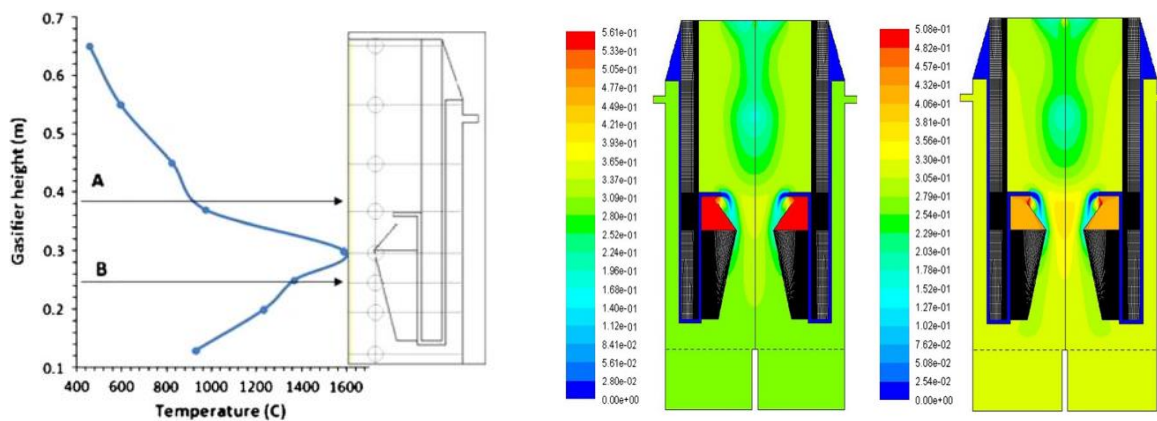


Figure 4. CFD temperature profile (left) and CFD contours profile of CO and H<sub>2</sub> (right)

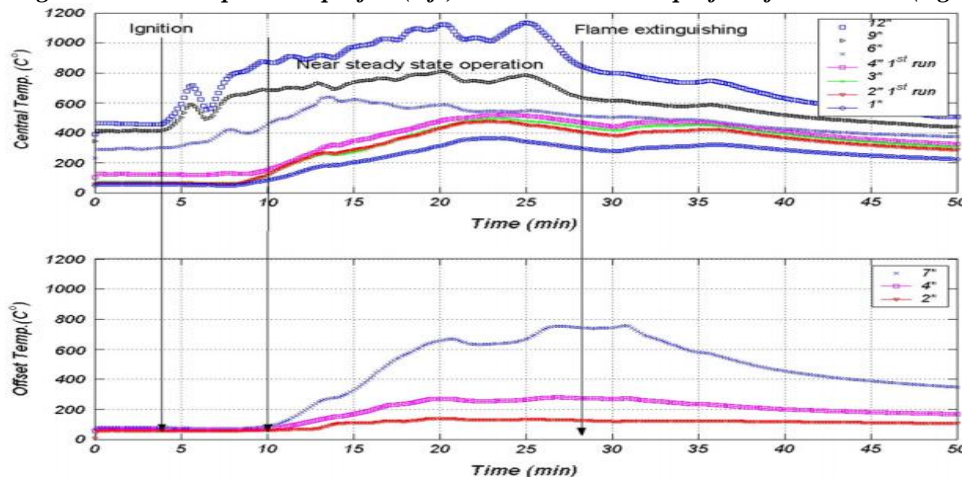


Figure 5. Temperature variation measured throughout the experiment by thermocouples placed through the gasifier center (above) and at 2.5'' (6.35 cm) offset from the center (below).

Various researches on the modeling and simulation of biomass gasifier shown in the table containing the example of CFD applications of biomass gasification and pyrolysis with the sub models used.

**Table 1. CFD Application In Biomass Gasification And Devolatilisation**

SN	Application	Code	Dim	Outcome/result	Turb. Model	Add. Model	Agreement with experiment	Reference/ authors
1	Downdraft gasifier	Fluent 14.5	2D	Effect of highly preheated air and steam	Std k-ε	Euler-Euler multiphase	Reasonable	Wu, Yueshi [19]
2	Two stage downdraft gasifier	Fluent	2D	To investigate in detail the oxidation zone; temperature profile; velocity pattern; tar conversion mechanism study	RNG k-ε	DOM	Satisfactory	Gerun, L [20]
3	Downdraft gasifier	Fluent 14.5	3D	Numerical model to investigate the thermal-hydraulic and gasification process	Std k-ε	P1 & DPM	n/a	Kanjariya, J. R. [21]
4	Downdraft gasifier	Fluent	2D	The factors affecting the producer gas such as equivalence ratio, gas composition, higher heating value and the temperature distribution inside the gasifier	RNG k-ε	Species transport model	satisfactory	Murugan, P. and S. J. Sekhar [22]
5	Downdraft gasifier	code	1D	Predictions of the gas composition and the axial temperature profile	n/a	n/a	Good	Di Blasi, [23]
6	Entrained Flow gasifier	CFX4	3D	products mass fraction distribution; temperature contours; swirl velocity distribution	Std k-ε RSM	lagrangian	Acceptable	Fletcher, D [24]
7	Entrained flow gasifier	Fluent	2D	To model gasification of petroleum residue for simulate the effects of equivalence ratio and pressure on carbon conversion efficiency, tar yield, hydrogen concentration, and higher heating value of the syngas	n/a	n/a	Good	Xiangyi, B [25]
8	Cross-type two-stage gasifier	Fluent	3D	effects of the O <sub>2</sub> /Coal ratio, coal slurry concentration, and 1st-2nd stage fuel distribution ratio on gasification performance	Std k-ε	Euler-Lagrangian, DPM, STM	Good	Luan, Y.-T [26]
9	Downdraft gasifier	Fluent	2D	Effect of porosity, oxidizer velocity and type of biomass fuels implications on the gasification zone and process in a downdraft gasifier of this design.	n/a	Non premixed model	n/a	Muilenburg, M. [27]
10	Downdraft gasifier	Code	3D	Pressure drop, temperature profile, model parametric analysis	n/a	Porous	n/a	Sharma, A. K. [28]
11	circulating fluidized-bed (CFB) reactor		2D	The impacts of turbulence models, radiation model, water-gas shift reaction, and equivalence ratio	Std k-ε	Eulerian-Eulerian, P1, Granual flow	Good	Liu, H [29]

Dim=Dimension, Turb=Turbulence, Std=Standard, DOM = Discrete Ordinates Model (radiation), DPM= Discrete Phase Model, STM= Species Transport Model,

## VI. CONCLUSION

The purpose of this paper has been to review the various research works on mathematical models, simulation models, heat integration, co-firing and enhancement which are contributing to the development of synthesis gas as an energy carrying clean fuel. From this review of literatures, the following conclusions can be drawn

- ➔ Different type of mathematical and numerical model used in CFD analysis of biomass conversion process (gasification and combustion) using different type of computer application fluent, CFX and code modeling etc. and investigate their computation result with the experimental result.
- ➔ Effect of different type of parameter as the type of fuel, oxidizer velocity, equivalence ratio, pressure, porosity etc. in gasification process.
- ➔ Various modeling approaches discussed have their own strengths and limitations. Mathematical models are necessary for the optimization purposes to find optimal operating conditions which obtain better process performance.
- ➔ CFD models are also one of the tools to develop 2D and 3D models with better accuracy but it requires lot of kinetic and design data from the literature.

## REFERENCES

1. Saidur, R., et al., *A review on biomass as a fuel for boilers*. Renewable and sustainable energy reviews, 2011. **15**(5): p. 2262-2289.
2. *biomass power/cogen*. 2012; Available from: <http://mnre.gov.in/schemes/grid-connected/biomass-powercogen>.
3. Wang, Y. and L. Yan, *CFD studies on biomass thermochemical conversion*. International journal of molecular sciences, 2008. **9**(6): p. 1108-1130.
4. McKendry, P., *Energy production from biomass (part 1): overview of biomass*. Bioresource technology, 2002. **83**(1): p. 37-46.
5. McKendry, P., *Energy production from biomass (part 3): gasification technologies*. Bioresource technology, 2002. **83**(1): p. 55-63.
6. Kishore, V., *Renewable energy engineering and technology: a knowledge compendium*. 2008: Energy and Resources Institute.
7. Anderson, J.D. and J. Wendt, *Computational fluid dynamics*. Vol. 206. 1995: Springer.
8. Pallarés, J., et al., *Numerical study of co-firing coal and Cynara cardunculus in a 350 MWe utility boiler*. Fuel Processing Technology, 2009. **90**(10): p. 1207-1213.
9. Launder, B.E. and D.B. Spalding, *Lectures in mathematical models of turbulence*. 1972.
10. Shih, T.-H., et al., *A new k- $\epsilon$  eddy viscosity model for high reynolds number turbulent flows*. Computers & Fluids, 1995. **24**(3): p. 227-238.
11. Magnussen, B.F. and B.H. Hjertager. *On mathematical modeling of turbulent combustion with special emphasis on soot formation and combustion*. in *Symposium (international) on Combustion*. 1977. Elsevier.
12. Habibi, A., B. Merci, and G.J. Heynderickx, *Impact of radiation models in CFD simulations of steam cracking furnaces*. Computers & chemical engineering, 2007. **31**(11): p. 1389-1406.
13. Yu, J., et al., *Biomass pyrolysis in a micro-fluidized bed reactor: characterization and kinetics*. Chemical engineering journal, 2011. **168**(2): p. 839-847.
14. Pratt, D.T., L. Smoot, and D. Pratt, *Pulverized coal combustion and gasification*. Vol. 8. 1979: Springer.
15. Govind, R. and J. Shah, *Modeling and simulation of an entrained flow coal gasifier*. AIChE Journal, 1984. **30**(1): p. 79-92.
16. Kaushal, P., T. Pröll, and H. Hofbauer, *Model development and validation: co-combustion of residual char, gases and volatile fuels in the fast fluidized combustion chamber of a dual fluidized bed biomass gasifier*. Fuel, 2007. **86**(17): p. 2687-2695.
17. Gómez-Barea, A. and B. Leckner, *Modeling of biomass gasification in fluidized bed*. Progress in Energy and Combustion Science, 2010. **36**(4): p. 444-509.
18. Janajreh, I. and M. Al Shrah, *Numerical and experimental investigation of downdraft gasification of wood chips*. Energy Conversion and Management, 2013. **65**: p. 783-792.
19. Wu, Y., et al., *Two-dimensional computational fluid dynamics simulation of biomass gasification in a downdraft fixed-bed gasifier with highly preheated air and steam*. Energy & Fuels, 2013. **27**(6): p. 3274-3282.
20. Gerun, L., et al., *Numerical investigation of the partial oxidation in a two-stage downdraft gasifier*. Fuel, 2008. **87**(7): p. 1383-1393.
21. Kanjariya, J.R., R.N. Patel, and A.M. Lakdawala. *Numerical simulation and modeling of a downdraft gasifier*. in *Multi-disciplinary Sustainable Engineering: Current and Future Trends: Proceedings of the 5th Nirma University International Conference on Engineering, Ahmedabad, India, November 26-28, 2015*. 2016. CRC Press.
22. Murugan, P. and S.J. Sekhar, *Species-Transport CFD model for the gasification of rice husk (Oryza Sativa) using downdraft gasifier*. Computers and Electronics in Agriculture, 2017. **139**: p. 33-40.
23. Di Blasi, C., *Dynamic behaviour of stratified downdraft gasifiers*. Chemical engineering science, 2000. **55**(15): p. 2931-2944.

24. Fletcher, D., et al., *A CFD based combustion model of an entrained flow biomass gasifier*. Applied mathematical modelling, 2000. **24**(3): p. 165-182.
25. Xiangyi, B., et al., *CFD simulation of entrained-flow gasification of liquid fuels*. Petroleum Science and Technology, 2016. **34**(19): p. 1642-1646.
26. Luan, Y.-T., Y.-P. Chyou, and T. Wang, *Numerical analysis of gasification performance via finite-rate model in a cross-type two-stage gasifier*. International Journal of Heat and Mass Transfer, 2013. **57**(2): p. 558-566.
27. Muilenburg, M., Y. Shi, and A. Ratner. *Computational modeling of the combustion and gasification zones in a downdraft gasifier*. in *ASME 2011 International Mechanical Engineering Congress and Exposition*. 2011. American Society of Mechanical Engineers.
28. Sharma, A.K., *Modeling fluid and heat transport in the reactive, porous bed of downdraft (biomass) gasifier*. International Journal of Heat and Fluid Flow, 2007. **28**(6): p. 1518-1530.
29. Liu, H., et al., *Computational fluid dynamics modeling of biomass gasification in circulating fluidized-bed reactor using the Eulerian–Eulerian approach*. Industrial & Engineering Chemistry Research, 2013. **52**(51): p. 18162-18174.